Spin-polarized transport across a $La_{0.7}Sr_{0.3}MnO_3/YBa_2Cu_3O_{7-x}$ interface: Role of Andreev bound states

Z. Y. Chen,* Amlan Biswas, Igor Žutić, T. Wu, S. B. Ogale, R. L. Greene, and T. Venkatesan*

Center for Superconductivity Research, Department of Physics, University of Maryland, College Park, Maryland 20742

(Received 20 June 2000; published 7 May 2001)

Transport across an $La_{0.7}Sr_{0.3}MnO_3/YBa_2Cu_3O_{7-x}$ (LSMO/YBCO) interface is studied as a function of temperature and surface morphology. For comparison, control measurements are performed in nonmagnetic heterostructures of $LaNiO_3$/YBCO and Ag/YBCO. In all cases, YBCO is used as bottom layer to eliminate the channel resistance and to minimize thermal effects. The observed differential conductance reflects the role of Andreev bound states in the *a-b* plane, and displays the suppression of such states by the spin-polarized transport across the interface. The theoretical analysis of the measured data reveals decay of the spin polarization near the LSMO surface with temperature, consistent with the reported photoemission data.

DOI: 10.1103/PhysRevB.63.212508 PACS number(s): 74.50.+r, 75.70.Rf, 75.70.Cn

The pioneering work on spin-polarized transport in conventional superconductors,[1] performed in the tunneling limit of strong interfacial scattering, has been recently extended to high transparency ferromagnet-superconductor heterostructures,[2,3] where the two-particle process of Andreev reflection plays an important role. There is generally a good understanding of transport in normal-metal–high-temperature-superconductor (HTSC) junctions and the important role of the Andreev bound states (midgap states),[4–8] which lead to the formation of the zero bias conductance peak (ZBCP). In contrast, there remain many open questions in the spin-polarized case involving heterostructures of colossal magnetoresistance materials (CMR) and HTSC.[9–12] Systematic studies of these systems with high spin polarization are particularly important as they hold potential for probing ferromagnetic interfaces, unconventional superconductivity,[11,12] and for modifying superconducting properties, such as the critical current and superconducting transition temperature, T_c.[9] Understanding and control of interface properties in CMR/HTSC heterostructures could also lead to novel spin-based devices. The key factors in such studies are the electronic and magnetic quality of the interface region on the sides of the ferromagnet and the superconductor, and the thermal management of the device configuration, since these can critically influence the outcome of the measurement.

In this work we report and analyze some observations of spin-polarized transport at a high quality $La_{0.7}Sr_{0.3}MnO_3/YBa_2Cu_3O_{7-x}$ (LSMO/YBCO) interface. In contrast to previous studies,[10,13] YBCO is used as the bottom electrode. This choice of geometry [Fig. 1(a)] eliminates the channel resistance and minimizes heating effects, thereby unfolding some peculiar features in the differential conductance-voltage (*G-V*) characteristics, not reported so far. By analyzing these features we are able to show that the Andreev bound states, observed in the *a-b* plane HTSC tunneling experiments,[5,6] have a major influence on the transport properties across the CMR/HTSC interface. These results also reveal the suppression of such bound states by the spin-polarized transport across the interface, as predicted theoretically.[11,12] Our analysis of the interfacial spin polarization is consistent with the findings of photoemission experiments, which show that the surface spin polarization of LSMO decreases more rapidly with temperature than that of the bulk.[14]

All films involved in the measurement were made by the pulsed laser deposition (PLD) technique. Before we address the issue of high quality film growth it is helpful to discuss our testing structure, shown in Fig. 1(a). Several important considerations were involved in fabricating this seemingly simple structure to achieve high-quality and reproducibility of the results. In particular, the use of $YBa_2Cu_3O_{7-x}$ as the bottom layer offers three significant advantages. (a) Eliminating the channel resistance contribution at temperatures below the T_c of YBCO. Thus, the CMR/HTSC interface contribution dominates the resistance. (b) Providing an equipotential surface leading to a uniform and perpendicular current distribution. (c) Avoiding heating effects from the CMR layer, which is significant in other structures. Au pads of 150×200 μm separated by 500 μm were patterned using optical lithography, and ion milled down to the YBCO layer in Argon ambient.[15] In order to ensure absence of possible shorting, the YBCO layer was always 15% overetched. 25-μm-thick gold wires were directly bonded to the top gold contact layer for measurements of current-voltage characteristic in a four-probe configuration. The results of such measurements were differentiated digitally to extract *G-V* curves. In the PLD procedure: first, a 2000 Å film of *c*-axis YBCO was grown on a (100) $SrTiO_3$ substrate using an energy density of 1.7 J/cm^2 in O_2 pressure of 150 Mtorr at 800 °C giving a T_c of 90 K. A 700 Å film of LSMO was then deposited on the YBCO layer using an energy density of 2 J/cm^2 in 400 mtorr O_2 at 780 °C and the structure was allowed to cool naturally in 400 Torr O_2. Finally, 200 Å gold was deposited *in situ* in a vacuum of 1×10^{-6} Torr at 90 °C to protect the surface, followed by another *ex situ* deposition of a 3000 Å Au layer by thermal evaporation. Rocking curves routinely have full width of half maximum of less than 0.3° for both YBCO and LSMO peaks, indicating the high quality of the films produced by this procedure. After all the processing steps the T_c of the YBCO films

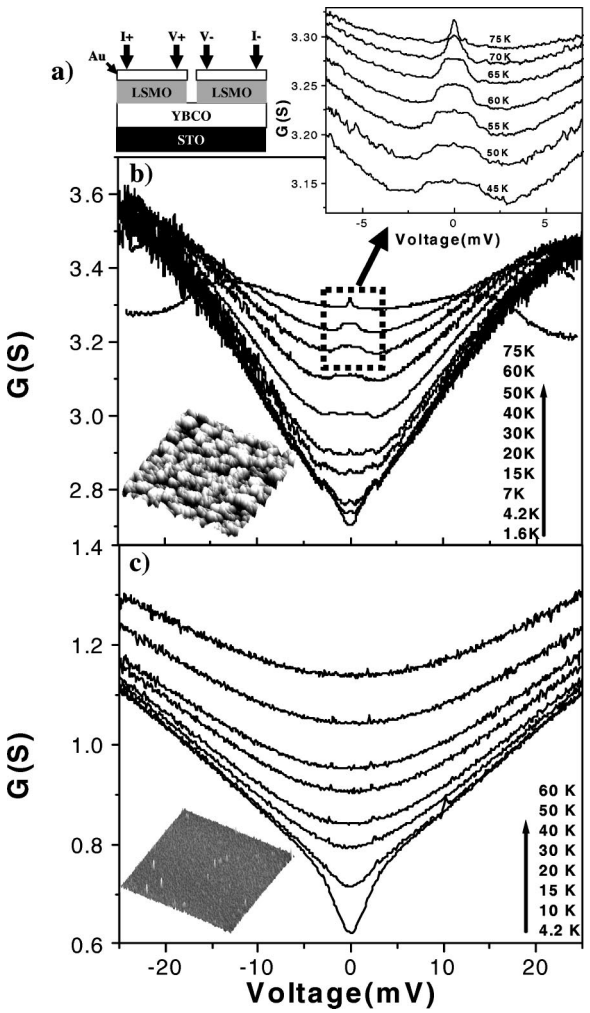

FIG. 1. (a) Testing structure for LSMO/YBCO junction. (b) Raw conductance data at various temperatures as a function of applied voltage for two different surface morphologies with the corresponding atomic force microscope (AFM) images representing 5×5 μm scan size and same height range. In (b) optimally grown YBCO ($T_c=90$ K) and in (c) smoother, off-optimal YBCO ($T_c=83$ K).

remains 90 K. We performed a similar experiment on much smoother YBCO films, specifically grown under slightly off-optimum conditions[16] (substrate temperature: 780 °C, energy density: 1.4 J/cm^2). Although the T_c in this case was only 7 K lower, the surface morphology was considerably flatter, as shown in the insets of Fig. 1(b) and 1(c).

The resistance of the LSMO/YBCO junction is composed of three parts: the Au/LSMO interface, the LSMO electrode, and the LSMO/YBCO interface. According to the literature,[17] even an *ex situ* grown Au/LSMO interface has a surface resistivity of about 1×10^{-6} Ω cm^2 at room temperature, hence the resistance coming from the Au/LSMO interface in our case is smaller than 3.3 mΩ. Taking a very conservative estimate for the resistivity of LSMO as 10 mΩ cm, we conclude that the LSMO electrode has a resistance of about 2.3 mΩ. Given that the total resistance in our structure is about 300 mΩ, these parasitic resistances can be neglected and the G-V curves below T_c can be regarded as genuinely representing the properties of the LSMO/YBCO interface.

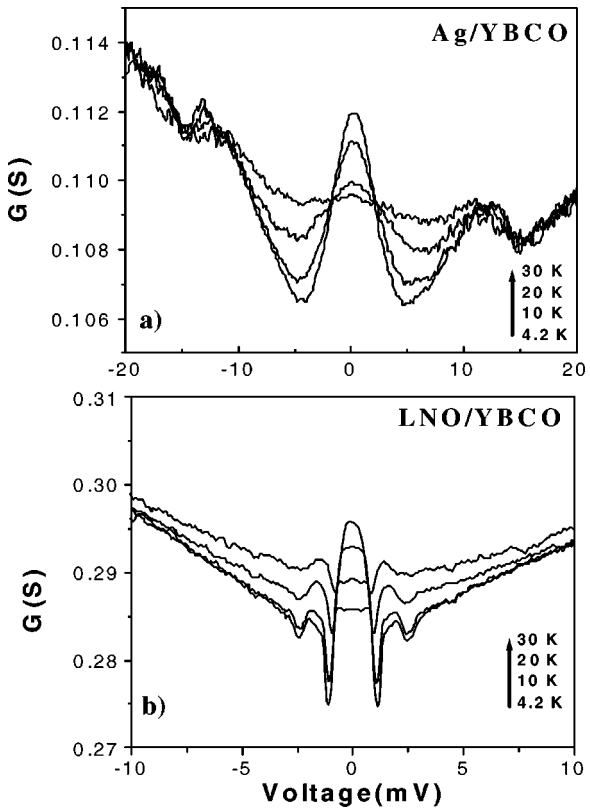

FIG. 2. Temperature evolution of G-V data for (a) Ag/YBCO and (b) LNO/YBCO junction. Both panels display ZBCP for a *c*-axis grown YBCO.

The conductance data, shown for the ''faceted'' [Fig. 1(b)][18] and smooth [Fig. 1(c)] interface, display a general ''V''-shaped background, similar to the tunneling data in metallic oxide systems.[19,20] The G-V curves were seen to converge at higher bias in all the data up to 85 K, indicating that there is little contribution from the YBCO channel over this temperature range. Similarly, we can argue that the thermal effects are minimized. The change of curvature in Fig. 1(b) at higher voltages around 60 K can be explained by the presence of vortices when the channel current approaches the critical current. The most significant difference between the two sets of data is the structure near the zero bias in Fig. 1(b). At higher temperatures it evolves into ZBCP, but is completely absent for the smoother surface in Fig. 1(c). We attribute the possibility to observe ZBCP in our *c*-axis oriented film to the known interfacial roughness of optimally grown YBCO which facilitates *a*-*b* plane transport. Consequently, such surface morphology, due to the sign change of *d*-wave order parameter would introduce nonvanishing weight of the *a*-*b* plane Andreev bound states.[7,8] To investigate this point we perform control measurements with nonmagnetic systems in the geometry[21] shown in Fig. 1(a) where LSMO is replaced by LNO [Fig. 2(a)] and by Ag [Fig. 2(b)]. In spite of the significantly different electronic properties of LNO and Ag, conductance data in both cases display similar behavior: a ZBCP, present already at lowest examined temperature diminishes at higher temperature, consistent with the effects of thermal smearing. These measurements (in par-

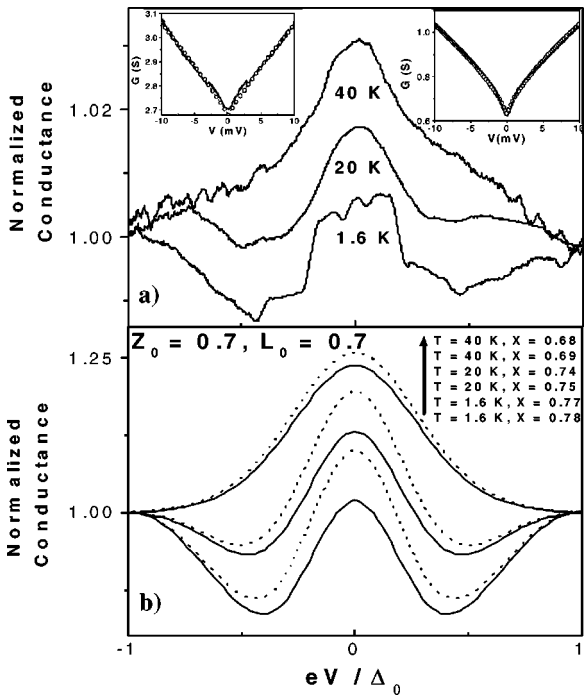

FIG. 3. (a) Normalized conductance after removing the contribution of the CMR DOS. (b) Calculated results, averaged over all interfacial orientations. For comparison, at each temperature in panel (a), two curves with slightly different spin polarization are shown. The notation is following Ref. 12. Insets show curves fitted at the lowest examined temperature to include the effects of the CMR DOS. Fitting parameters, as explained in the text, are $G_0 = 2.68$ S, $\Delta = 0.058$ meV, $n = 0.913$ (left inset) for a faceted surface, and $G_0 = 0.62$ S, $\Delta = 0.017$ meV, $n = 0.743$ (right inset) for a smooth surface.

ticular the one on LNO which, as a metallic oxide, is similar to LSMO) allow us to investigate the distinguishing conductance features arising from the spin-polarized transport.

In order to reveal the properties of interface transport from Fig. 1(b) near zero bias with greater clarity, we have to distinguish between the contributions of the two electrodes of the junction, to the G-V curves. Since we are mainly interested in studying the effect of spin polarized tunneling into the HTSC, we would like to remove the effect of the complicated density of states (DOS) of the CMR electrode from the raw conductance data. The DOS of CMR have been studied by tunneling spectroscopy[22–24] leading to the corresponding conductance contribution at low bias given by $G(V) = G_0(1 + (|eV|/\Delta)^n)$, where G_0 is the zero bias value, Δ is the correlation gap, and $0.5 < n < 1$. To determine background conductance (assuming that it is predominantly due to the CMR DOS), which should be removed from the measured G-V curves, we first fit $G(V)$ to the data at lowest T and next, for each higher T, apply thermal smearing to the fitted curve.[25] The resulting curves, after removing background conductance at three different temperatures, are shown in Fig. 3(a).[26] Each curve is normalized with respect to its value at Δ_0, corresponding to the maximum gap.[6] We compare these results with the theoretical analysis for transport across CMR/HTSC junction by adopting the notation and methods from Ref. 12, generalized to finite temperature. The strength of interfacial scattering is modeled by parameter Z_0 and the spin polarization is represented by X, the ratio of the exchange and Fermi energies for CMR. The limit $X = 0$ depicts the unpolarized case, while $X = 1$ corresponds to the complete polarization of a half-metallic ferromagnet. To include the effects of different electronic densities in the two materials, we use L_0, the ratio of Fermi wavevectors in HTSC and CMR.[27] Additionally, to capture the main aspects of surface roughness, we average results over different interface orientations. This is in contrast to the usually studied extreme cases of (110) and (100) planes, corresponding to the maximum and minimum spectral weight of the Andreev bound states, respectively. The calculated conductance is normalized with respect to its value at the maximum gap.

For each G-V curve from Fig. 3(a), we plot in Fig. 3(b) two curves for corresponding temperature with slightly different values of X, to illustrate the sensitivity of results to the spin polarization of a ferromagnet. We show that the the essential features from Fig. 3(a) are well reproduced. The overall amplitude is expected to be much smaller from measured values since in the analysis we do not include c-axis contribution which could be modeled by a parallel conductance channel.[6] Findings from Fig. 3(b) (which we have also verified in a wide parameter range) show that at a fixed temperature the increase in the exchange energy reduces the amplitude of ZBCP. This can partly explain smaller magnitude of ZBCP observed in LSMO/YBCO as compared to the nonmagnetic junctions. Another influence, contributing to this difference in magnitude, could arise from the previously discussed DOS effect of the CMR electrode. Using the theoretical framework from Refs. 11,12 it is possible to understand various effects on conductance data from the temperature dependent exchange interaction responsible for the spin subband splitting and the spin polarization in the ferromagnetic region. In the limit of low T and almost complete spin polarization it is predicted that there would be a strong conductance suppression at low bias voltage where the transport properties are governed by Andreev reflection. For spin-polarized carriers only a fraction of the incident electrons from a majority spin subband will have partner from a minority spin subband in order to be Andreev reflected, leading to a reduced charge transport across the interface.[2,11,12,28] If the spin-polarization decreases with temperature there would be a smaller difference between population in the two spin subbands resulting in an enhanced Andreev reflection and more pronounced ZBCP. This temperature dependence is qualitatively different from the effects of thermal smearing which reduce and broaden ZBCP. Our raw data, from the blow up in Fig. 1(b), provides therefore a strong support for the decreasing spin polarization with temperature which can even be sufficiently fast to offset the opposite effects of thermal smearing. Observing ZBCP at temperatures close to T_c further suggests that fabricating our junctions have provided high interfacial quality without degrading the superconducting properties. From the calculated conductance we could infer high, but not complete, spin polarization at lowest measured temperature, which is consistent with several other findings using different techniques.[3,29] A detailed study on

the LSMO/YBCO interface by x-ray magnetic circular dichroism[30] has concluded that the polarization of LSMO is further suppressed, compared to the free surface, by the presence of a capping YBCO layer. In the case of LSMO, this should serve as a caution for attempts to get the precise quantitative agreement in the degree of spin polarization obtained by various measurement techniques which often also involve different material fabrication. The temperature dependence of the spin polarization from our data is consistent with the results of spin-resolved photoemission spectroscopy data,[14] which show that the spin polarization within 50 Å of the free surface of LSMO drops faster than the bulk with increasing temperature.

In conclusion, by controlling the surface morphology in a *c*-axis grown YBCO we have demonstrated qualitatively different temperature evolution of the measured conductance features in the ferromagnetic and nonmagnetic superconducting heterostructures. These differences are attributed to the suppression of the spectral weight of the Andreev bound states by the spin-polarized transport across the interface.

This work was supported by the US ONR Grants No. N000140010028, N000149810218, the NSF MRSEC Grant No. DMR-00-80008, and by DARPA. We thank P. Fournier, I. I. Mazin, B. Nadgorny, and I. Takeuchi for valuable discussions.

*Also at Department of Electrical Engineering, University of Maryland, College Park.

[1] R. Meservey and P.M. Tedrow, Phys. Rep. **238**, 173 (1994).
[2] M.J.M. de Jong and C.W.J. Beenakker, Phys. Rev. Lett. **74**, 1657 (1995).
[3] R.J. Soulen, Jr. *et al.*, Science **282**, 85 (1998); S.K. Upadhyay *et al.*, Phys. Rev. Lett. **81**, 3247 (1998).
[4] C.R. Hu, Phys. Rev. Lett. **72**, 1526 (1994); Phys. Rev. B **57**, 1266 (1998); Y. Tanaka and S. Kashiwaya, Phys. Rev. Lett. **74**, 3451 (1995).
[5] M. Covington *et al.*, Phys. Rev. Lett. **79**, 277 (1997); S. Sinha and K.-W. Ng, *ibid.* **80**, 1296 (1998); J.Y.T. Wei *et al.*, *ibid.* **81**, 2542 (1998); R. Krupke and G. Deutscher, *ibid.* **83**, 4634 (1999).
[6] Y. Dagan *et al.*, Phys. Rev. B **61**, 7012 (2000).
[7] M. Fogelström *et al.*, Phys. Rev. Lett. **79**, 281 (1997).
[8] M.B. Walker and P. Pairor, Phys. Rev. B **60**, 10 395 (1999).
[9] V.A. Vas'ko *et al.*, Phys. Rev. Lett. **78**, 1134 (1997); Z.W. Dong *et al.*, Appl. Phys. Lett. **71**, 1718 (1997); N.-C. Yeh *et al.*, Phys. Rev. B **60**, 10 522 (1999); A.M. Goldman *et al.*, J. Magn. Magn. Mater. **200**, 69 (1999).
[10] V.A. Vas'ko *et al.*, Appl. Phys. Lett. **73**, 844 (1998).
[11] J.X. Zhu *et al.*, Phys. Rev. B **59**, 9558 (1999); I. Žutić and O.T. Valls, *ibid.* **60**, 6320 (1999); S. Kashiwaya *et al.*, *ibid.* **60**, 3572 (1999).
[12] I. Žutić and O.T. Valls, Phys. Rev. B **61**, 1555 (2000).
[13] A. Sawa *et al.*, cond-mat/9908431 (unpublished).
[14] J.-H. Park *et al.*, Phys. Rev. Lett. **81**, 1953 (1998).
[15] Although the junction size we use is large compared to the mean free path of the electrons, it was both shown experimentally (Refs. 5,13), and predicted theoretically (Ref. 8) that a ZBCP can still be observed in the diffusive limit.
[16] It is known that off-stoichiometric phases that may be segregated into grain boundaries or the surface under optimized, well-equilibrated conditions cause large surface roughness. Under off-optimal conditions, segregation is suppressed by the process of incorporation of defects into the lattice, which also leads to a smoother surface.
[17] L. Mieville *et al.*, Appl. Phys. Lett. **73**, 1736 (1998).
[18] We also performed these transport measurements with magnetic fields parallel to the interface. No significant anisotropy was observed for different directions of the applied field.
[19] J.Z. Sun *et al.*, Appl. Phys. Lett. **73**, 1008 (1998).
[20] A.K. Raychaudhuri *et al.*, Physica B **51**, 7421 (1995); M. S. Rzchowski *et al.* (unpublished); A.K. Raychaudhuri, Adv. Phys. **44**, 21 (1996).
[21] The actual pad size is 15×15 μm, smaller than for the LSMO/YBCO junction, to obtain a sufficiently large signal.
[22] A. Tiwari and K.P. Rajeev, Phys. Rev. B **60**, 10 591 (1999).
[23] A. Biswas *et al.*, Phys. Rev. B **59**, 5368 (1999).
[24] J.Y.T. Wei *et al.*, Phys. Rev. Lett. **79**, 5150 (1997).
[25] For T above 40 K this procedure could not be simply implemented because of the emergence and strengthening of winglike features at higher bias.
[26] Applying this procedure on the raw data from Fig. 1(c) gave no discernible features in conductance curves.
[27] Considering reported values for Fermi velocities in LCMO [W.E. Pickett and D.J. Singh, Phys. Rev. B **53**, 1146 (1996)] and in YBCO [K. Krishna, J.M. Haris, and N.P. Ong, Phys. Rev. Lett. **75**, 3529 (1995)], we can infer that $L_0<1$. Our choice of $L_0=0.7$ preserves well all the conductance features for calculated curves with $L_0=1$, assuming no Fermi wave vector mismatch.
[28] I. Žutić and S. Das Sarma, Phys. Rev. B **60**, R16 322 (1999).
[29] D.C. Worledge and T.H. Geballe, Appl. Phys. Lett. **76**, 900 (2000).
[30] S. Stadler *et al.*, Appl. Phys. Lett. **75**, 3384 (1999).